Journal of Alloys and Compounds 509 (2011) 1824–1829

Contents lists available at ScienceDirect

Journal of Alloys and Compounds

journal homepage: www.elsevier.com/locate/jallcom

Microstructure, dielectric and ferroelectric properties of $0.94Bi_{0.5}Na_{0.5}TiO_3$–$0.06BaTiO_3$ (NBTB) and $0.05BiFeO_3$–0.95NBTB ceramics: Effect of sintering atmosphere

XiaoMing Chen*, WenYue Pan, HuanHuan Tian, XuXu Gong, XiaoBing Bian, Peng Liu

College of Physics and Information Technology, Shaanxi Normal University, 199 South Chang'an Road, Xi'an 710062, Shaanxi, People's Republic of China

ARTICLE INFO

Article history:
Received 25 August 2010
Received in revised form 8 October 2010
Accepted 9 October 2010
Available online 12 November 2010

Key words:
Ceramics
Microstructure
Electronic properties
Sintering atmospheres

ABSTRACT

$0.94Bi_{0.5}Na_{0.5}TiO_3$–$0.06BaTiO_3$ (NBTB) and $0.05BiFeO_3$–0.95NBTB (BF-doped NBTB) lead-free ceramics were prepared by solid state reaction method. The ceramics were sintered at 1180 °C for 2 h in O_2 and N_2. All ceramics exhibited a single phase of perovskite structure. Relative amount of tetragonal phase was related to the sintering atmospheres. Both grain size and shape were influenced by the sintering atmospheres. Sintering the ceramics in N_2 weakened their dielectric anomalies corresponding to the transition from ferroelectric phase to the so-called "intermediate phase". When the NBTB and BF-doped NBTB ceramics were sintered in N_2, their maximum dielectric constant and the degree of diffuseness of the transition from the "intermediate phase" to paraelectric phase increased, but their Curie temperatures decreased. The difference in dielectric properties of the ceramics sintered in different atmospheres was closely related to the difference in oxygen vacancy concentration. The correlation between ferroelectric properties and sintering atmospheres is associated with a competing effect among oxygen vacancy concentration, A-site vacancy concentration and percentage of tetragonal phase.

1. Introduction

Among lead-free ferroelectric materials, $(1-x)Bi_{0.5}Na_{0.5}TiO_3$–$xBaTiO_3$-based ceramics have been studied widely because there exists a rhombohedral–tetragonal morphotropic phase boundary (MPB) near $x = 0.06$ [1–13]. The excellent electrical properties of the $(1-x)Bi_{0.5}Na_{0.5}TiO_3$–$xBaTiO_3$-based ceramics are always attributed to $(Bi_{0.5}Na_{0.5})^{2+}$ ions, especially Bi^{3+} ions, at the A-site of ABO_3 perovskite structure [14]. So, addition of other Bi-based ferroelectrics could possibly improve the performances of $Bi_{0.5}Na_{0.5}TiO_3$-based ceramics. Bismuth ferrite ($BiFeO_3$) is a ferroelectric with ABO_3 perovskite structure and high Curie temperature [15]. Doping of $BiFeO_3$ into $Bi_{0.5}Na_{0.5}TiO_3$-based ceramics can influence microstructures and electrical properties of the ceramics [16–20]. We have studied the effects of $BiFeO_3$ on microstructures, dielectric and ferroelectric properties of $0.94Bi_{0.5}Na_{0.5}TiO_3$–$0.06BaTiO_3$ (NBTB) ceramics [20]. Doping of $BiFeO_3$ into the NBTB ceramics created oxygen vacancies. However, the effects of oxygen vacancies on microstructures and electrical properties of the NBTB and $BiFeO_3$-doped NBTB ceramics remain unclear.

Oxygen vacancy plays a very important role in determining microstructures and electrical properties of oxide ceramics. It has been found that the structural transition of grain boundary and related grain growth behavior of $BaTiO_3$ ceramics were closely related to oxygen partial pressure during sintering [21]. Fisher et al. [22–24] found that the orthorhombic–tetragonal and tetragonal–cubic phase transitions of $(K_{0.5}Na_{0.5})NbO_3$ ceramics became more diffuse when they had a high oxygen vacancy concentration. Zhang et al. [25] found that sintering $(Ba_{0.95}Ca_{0.05})(Ti_{0.88}Zr_{0.12})O_3$ ceramics in a protective atmosphere could increase dielectric constants. Oxygen vacancies could restrain the phase transition between ferroelectric phase and the so-called "intermediate phase" in Mn-doped $(Na_{0.8}K_{0.2})_{0.5}Bi_{0.5}TiO_3$ ceramics [26]. The moving of domain walls in $BaTiO_3$ was also affected by oxygen vacancy defects [27]. In summary, oxygen vacancy is a very significant factor that can influence microstructures and electrical properties of ferroelectric ceramics.

In this paper, ceramics with compositions of $0.94Na_{0.5}Bi_{0.5}TiO_3$–$0.06BaTiO_3$ (NBTB) and $0.05BiFeO_3$–0.95NBTB (BF-doped NBTB) were sintered in atmospheres of O_2 and N_2. It can be expected that oxygen vacancy concentration would change with changing in compositions and sintering atmospheres. The effects of sintering atmospheres on microstructures, dielectric and ferroelectric properties of the NBTB and BF-doped NBTB ceramics were studied in detail.

* Corresponding author. Tel.: +86 29 85303823; fax: +86 29 85303823.
E-mail addresses: xmchen@snnu.edu.cn, xmchen-snnu@163.com (X. Chen).

0925-8388/$ – see front matter © 2010 Elsevier B.V. All rights reserved.
doi:10.1016/j.jallcom.2010.10.055

2. Experimental procedures

NBTB and BF-doped NBTB ceramics were prepared by solid state reaction method. Analytical grade $BaCO_3$, TiO_2, Na_2CO_3, Bi_2O_3, and Fe_2O_3 in stoichiometric ratio of the compositions were mixed in agate vials with agate balls and milled for 5 h in Fritsch Vario-Planetary high energy ball milling system in air. Rotation speed of the disk was 300 rpm and that of the vials was 450 rpm. The milled powders were subsequently calcined at 800 °C for 2 h. The calcined powders were pulverized with approximately 5 wt% polyvinyl alcohol. Pellets of 11.5 mm in diameter and approximately 1.5 mm in thickness were pressed at a uniaxial pressure of 200 MPa. The pellets were burned out the binder at 500 °C for 2 h, and sintered in atmospheres of O_2 and N_2. In order to obtain ceramics with coarse grains (>1 μm), samples were sintered at 1180 °C for 2 h. Heating and cooling rates were 3 °C/min. In order to prevent volatilization of Bi and Na, all pellets were embedded in powders with the same composition and placed in covered alumina crucibles during the sintering process.

X-ray diffraction (XRD, Rigaku D/Max 2550) using a Cu Kα radiation (40 kV and 50 mA) was used for identification of phase compositions. Microstructure of the sintered samples was observed by using scanning electron microscope (Quanta 200 SEM, FEI Co., Eindhoven, Netherlands). Average grain size was determined by the line intersect method. Density of all ceramics measured by Archimedes method was >94.6% of their corresponding theoretical density.

Silver electrodes were coated and fired at 650 °C for 15 min for electrical characterization. Dielectric measurement was performed by using an Agilent E4980A precision LCR from room temperature to 500 °C. Ferroelectric hysteresis loops were measured at 50 Hz in silicon oil with a radiant precision workstation ferroelectric testing system. Maximum polarization (P_m), remnant polarization (P_r) and coercive filed (E_c) were determined from the P–E hysteresis loops.

3. Results and discussion

Fig. 1(a) shows XRD patterns of the NBTB and BF-doped NBTB ceramics sintered in different atmospheres. All ceramics exhibit typical diffraction peaks of ABO_3 perovskite phase. No second phase is observed, suggesting that Bi^{3+} and Fe^{3+} ions have dissolved into the lattice structure of NBTB to form solid solutions.

As is known, a rhombohedral–tetragonal MPB exists in NBTB ceramics [28]. In order to characterize the phase compositions in a more quantitative way, the XRD peaks between 45.0° and 47.5° were fitted by Peakfit software using the least-square approach [20]. The XRD fitting patterns are shown in Fig. 1(b)–(e). The peaks between 45.0° and 47.5° were fitted into $(2\,2\,0)_T$ and $(2\,0\,2)_R$ peaks for all ceramics, where T and R denote tetragonal and rhombohedral phase, respectively. The results indicate that MPB appears in all samples. From the equation of tetragonal% = area $(2\,2\,0)_T$/(area $(2\,2\,0)_T$ + area $(2\,0\,2)_R$), relative amount of tetragonal phase was determined. They are 49.8%, 42.5%, 42.9% and 36.1% for the NBTB sintered in O_2, NBTB in N_2, BF-doped NBTB in O_2, and BF-doped NBTB in N_2, respectively. For the ceramics sintered in N_2, their relative amount of tetragonal phase decreases as compared to that of their counterparts sintered in O_2. For the ceramics sintered in same atmosphere, doping of $BiFeO_3$ into NBTB causes a decrease in percentage of tetragonal phase. XRD results show that MPB exists in the NBTB and BF-doped NBTB ceramics sintered in both atmospheres, but percentage of tetragonal phase is different for sample with different compositions and sintering atmospheres.

Fig. 2 shows SEM images of the NBTB and BF-doped NBTB ceramics sintered in different atmospheres. Average grain sizes of the NBTB ceramics sintered in O_2 and N_2 were determined to be 2.41 μm and 3.76 μm, respectively. For the BF-doped NBTB ceramics, mean grain sizes in O_2 and N_2 were 3.68 μm and 5.06 μm, respectively. The ceramics sintered in N_2 have larger grain size than those sintered in O_2. Grain growth was the most remarkable in the BF-doped NBTB ceramics sintered in N_2. On the other hand, the BF-doped NBTB ceramics sintered in N_2 consist of grains with round edges and corners, while the ceramics sintered in O_2 consist of cube-shaped grains with sharp edges and corners.

As reported in our previous work [20], Fe^{3+} ions should substitute Ti^{4+} ions in the $BiFeO_3$-doped NBTB ceramics. To maintain overall electrical neutrality, oxygen vacancies were created. Sintering the BF-doped NBTB ceramics in O_2 would decrease concentration of oxygen vacancies. It can be expected that oxygen vacancy concentration in the BF-doped NBTB ceramics sintered in N_2 is much higher than that in the ceramics sintered in O_2. As is generally recognized, the presence of oxygen vacancies in oxide materials is beneficial to mass transport during sintering. This should be responsible for the promoted grain growth in the ceramics sintered in N_2. It has been found that grain boundary structure and grain growth behavior of $BaTiO_3$ ceramics were affected by oxygen partial pressure [21]. Fisher and Kang [22] reported that the edge free energy of $(K_{0.5}Na_{0.5})NbO_3$ ceramics was reduced with increasing oxygen vacancy concentration, which caused a change in grain shape. We think that the change in grain shape in the BF-doped NBTB ceramics from cube to round with atmosphere changing from O_2 to N_2 is also related to an increase in oxygen vacancy concentration.

Fig. 3 shows variations in dielectric constant (ε_r) and dielectric loss ($\tan\delta$) of the NBTB and BF-doped NBTB ceramics sintered in different atmospheres as a function of temperature (T). ε_r at higher frequency is lower than that at lower frequency over the measured temperature range. For the ceramics sintered in both N_2 and O_2, the dependence of $\tan\delta$ on frequency is different over different temperature ranges, which is similar to that for the $BiFeO_3$-doped NBTB ceramics sintered in air [20]. Dielectric anomalies, caused by the phase transition between ferroelectric phase and the so-called "intermediate phase", were observed at about 150 °C (denoted as T_d peaks) in the NBTB and BF-doped NBTB ceramics sintered in O_2. But T_d peaks became vague when the two ceramics were sintered in N_2. Jiang et al. [26] reported that oxygen vacancies could restrain the transition of ferroelectric phase to the "intermediate phase" in Mn-doped $(Na_{0.8}K_{0.2})_{0.5}Bi_{0.5}TiO_3$ ceramics. As is known, sintering in O_2 would decrease oxygen vacancy concentration, while sintering in oxygen deficient atmosphere would increase oxygen vacancy concentration. Oxygen vacancies can cause domain wall clamping, which will restrain the macro-micro domain switching and inhibit the transition between ferroelectric phase and the "intermediate phase" [29]. Thus, the indistinctness of the T_d peaks for the ceramics sintered in N_2 can be attributed to their high concentrations of oxygen vacancy.

Dielectric peaks corresponding to maximum values of ε_r (denoted as ε_m) at Curie temperature (T_m) were observed in the ε_r–T curves. These peaks were caused by the phase transition between the "intermediate phase" and paraelectric phase. The values of ε_m and T_m for all ceramics measured at different frequencies are shown in Fig. 4. Sintering atmospheres have an important effect on both ε_m and T_m. ε_m of the ceramics sintered in N_2 is larger than that of the ceramics sintered in O_2 at a given frequency. That is to say, the samples sintered in an oxygen deficient atmosphere have higher ε_m values, which is always connected to electron relaxation polarization [25]. Similar phenomena were observed in $(BaCa)(TiZr)O_3$ [25] and Mn-doped $SrTiO_3$ ceramics [30].

T_m values of the ceramics sintered in N_2 decreased as compared to those of their counterparts sintered in O_2. In same sintering atmosphere, T_m of the BF-doped NBTB ceramics is larger than that of the NBTB ceramics. Many factors, such as grain size [31], secondary phase [32], crystal structure [33], and defect concentration [23,24,34], would result in a change in phase transition temperature. Uchino et al. [31] reported that T_m of $BaTiO_3$ decreased as the grain size dropped below 200 nm. In our work, the mean grain sizes in all samples are 2.41–5.06 μm, which are much larger than the particle sizes at which changes in T_m occur (Fig. 2). Therefore, it is unlikely that the change in grain size is the cause of the change in T_m. Lee et al. [32] explained the change in T_m of $BaTiO_3$ using the secondary phases on the surface of the perovskite crystals interacting elastically with the $BaTiO_3$. Here, no second phase was observed (Fig. 1). The decrease in tetragonality of $BaTiO_3$ can cause a decrease in T_m [33]. Härdtl and Wernickel [35] attributed the decrease in T_m

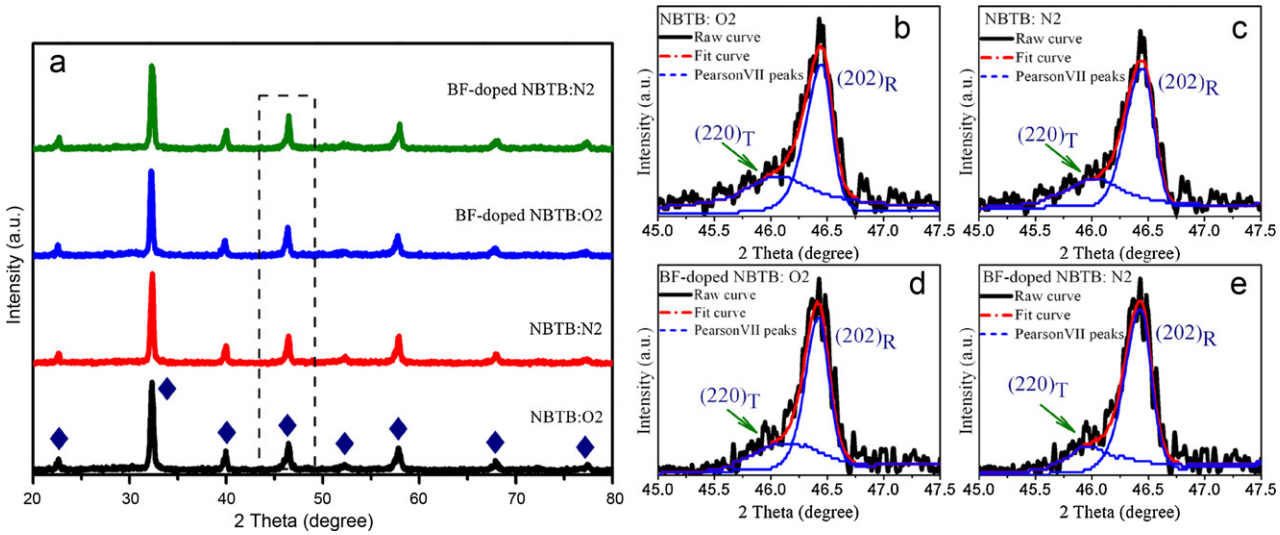

Fig. 1. XRD patterns of the NBTB and BF-doped NBTB ceramics sintered in different atmospheres (a), and fitted patterns of 45.0–47.5° (b–e). The symbol (♦) in (a) demonstrates perovskite structure.

of $BaTiO_3$ sintered in oxygen deficient atmosphere to the increased free electron concentration produced by the formation of oxygen vacancies or to changes in the lattice caused by oxygen vacancies. $(K_{0.5}Na_{0.5})NbO_3$ ceramics sintered in reducing atmospheres had lowered phase transition temperatures because of the increase in oxygen vacancy concentration [23,24]. Previous theoretical work [34] has also shown that a change in defect concentration would cause a change in phase transition temperature. In our previous work [20], we found that T_m of the $BiFeO_3$-doped NBTB ceramics sintered in air increased with increasing $BiFeO_3$ amount. Although oxygen vacancy concentration would increase by doping $BiFeO_3$, percentage of tetragonal phase decreased with increasing $BiFeO_3$ content. Variations in relative amount of tetragonal phase and oxygen vacancy concentration resulted in a change in T_m. Therefore, we think that the difference in T_m between the NBTB and BF-doped NBTB ceramics sintered in both N_2 and O_2 can be related to a competing effect between relative amount of tetragonal phase and oxygen vacancy concentration.

The dielectric behaviors with diffuse phase transition were further studied by fitting the results of temperature dependency

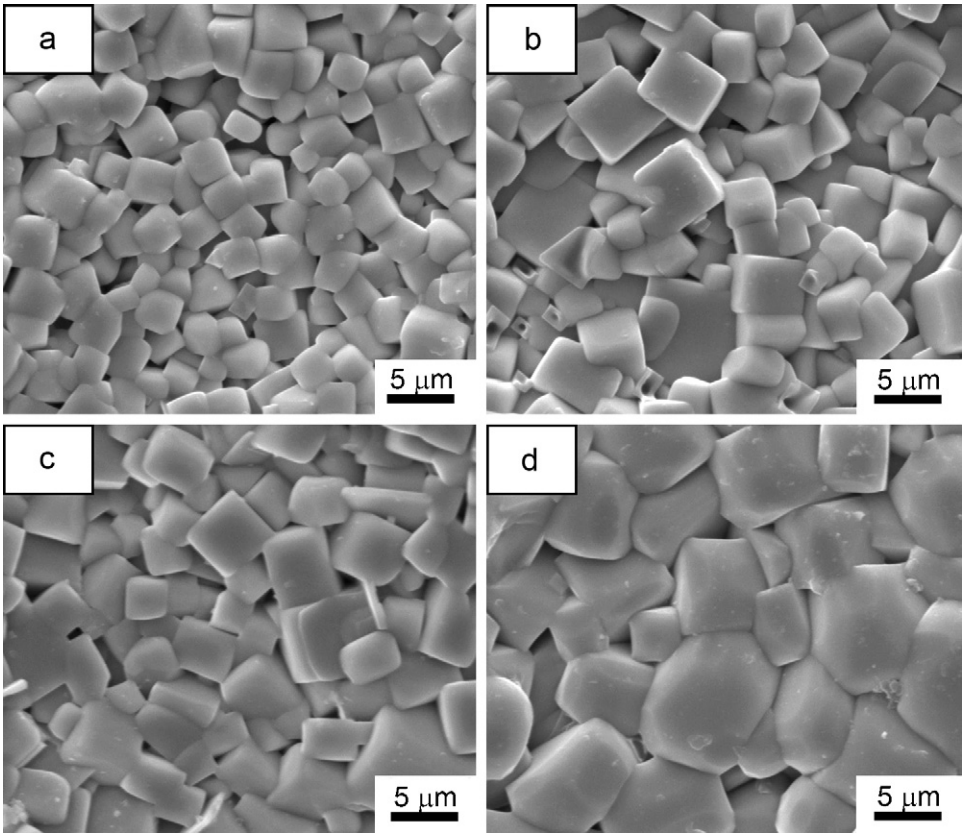

Fig. 2. SEM images of the NBTB ceramics sintered in O_2 (a), N_2 (b), and the BF-doped NBTB ceramics sintered in O_2 (c), and N_2 (d).

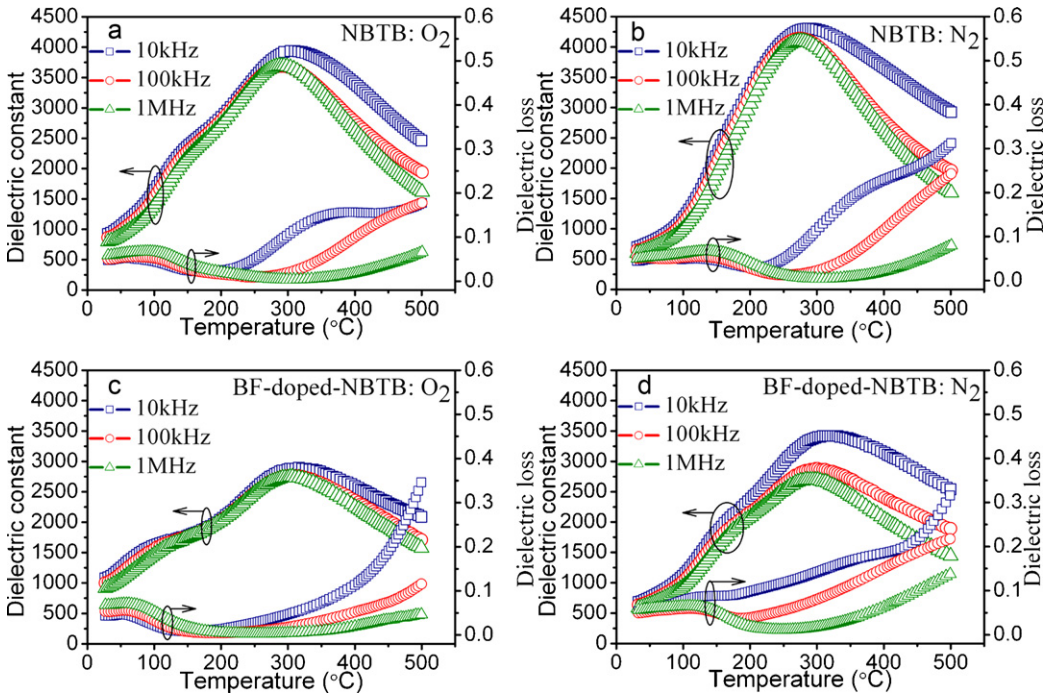

Fig. 3. Dielectric constant and dielectric loss of the NBTB and BF-doped NBTB ceramics sintered in different atmospheres versus temperature at frequencies of 10 kHz, 100 kHz and 1 MHz.

of dielectric constant to the modified Curie-Weiss law, which is described as [36]: $1/\varepsilon_r - 1/\varepsilon_m = (T - T_m)^\gamma/C'$, where ε_m is the maximum value of dielectric constant at phase transition temperature T_m, C' is Curie-like constant, and γ is the degree of diffuseness. γ is usually ranging from 1 for a normal ferroelectric to 2 for an ideal relaxor ferroelectric. Plots of $\mathrm{Ln}(1/\varepsilon_r - 1/\varepsilon_m)$ as a function of $\mathrm{Ln}(T - T_m)$ for all samples at frequencies of 10 kHz, 100 kHz and 1 MHz are shown in Fig. 5. All samples exhibit a linear characteristic. By least-square fitting the experimental data to the modified Curie–Weiss law, γ was determined. Because the diffuseness exponent γ of all samples is close to 2, the phase transition has a diffuse character. However, T_m does not exhibit obvious up-shift with increasing frequency for all samples (see Fig. 4(b)), which is different from classic relaxor characteristics [37]. γ of

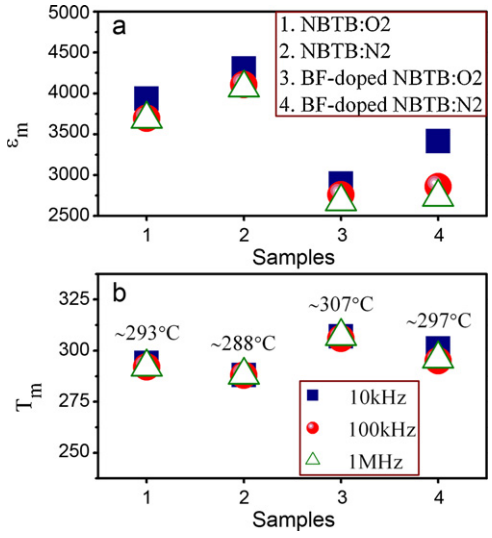

Fig. 4. Maximum values of dielectric constant (ε_m) and corresponding temperatures (T_m) for the NBTB and BF-doped NBTB ceramics sintered in different atmospheres.

the ceramics sintered in N_2 is higher than that of the ceramics sintered in O_2 at a given frequency. In same sintering atmosphere, γ of the NBTB ceramics is lower than that of the BF-doped NBTB ceramics at a given frequency. Therefore, with substitutions of Fe^{3+} ions for Ti^{4+} ions and an increase in oxygen vacancy concentration, the degree of diffuseness of the phase transition increased.

Fig. 6(a) shows polarization of the NBTB and BF-doped NBTB ceramics sintered in different atmospheres versus electric field measured at 50 Hz. Clear hysteresis loops were observed for all samples, which are typical shapes of ferroelectric materials. The remnant polarization (P_r), maximum polarization (P_m) and coercive field (E_c) of the samples were determined from their P–E hysteresis loops and are shown in Fig. 6(b). Both polarization and coercive field of the BF-doped NBTB ceramics are smaller than those of the NBTB ceramics sintered in same atmosphere. Compared with the ceramics sintered in O_2, those sintered in N_2 have smaller polarization and higher coercive filed.

Recently [20], we demonstrated that ferroelectric properties of the NBTB-based ceramics were determined by competitive factors, such as A-site vacancy, grain size, oxygen vacancy and percentage of tetragonal phase. Buessem et al. [38] reported that the coupling between grain boundaries and domain walls in fine-grained (1 μm or less) ceramics was stronger than that in coarse-grained ones. The stronger the coupling is, the weaker the ferroelectric properties are because of the decrease in domain wall mobility and achievable domain alignment. In this work, the sintering temperature was 1180 °C and the samples have coarse grains with mean sizes of 2.41–5.06 μm (Fig. 2). The grains are so large (≫1 μm) that the effects of coupling between grain boundaries and domain walls on ferroelectric properties of the ceramics can be neglected. Shigemi and Wada [39] found that the formation energy of Na vacancy was the lowest in oxidation atmosphere and that of O vacancy was the lowest in reduction atmosphere. Therefore, the ceramics sintered in O_2 would have increased concentrations of A-site vacancy and decreased concentrations of oxygen vacancy. The concentration of oxygen vacancy in the BF-doped NBTB ceramics sintered

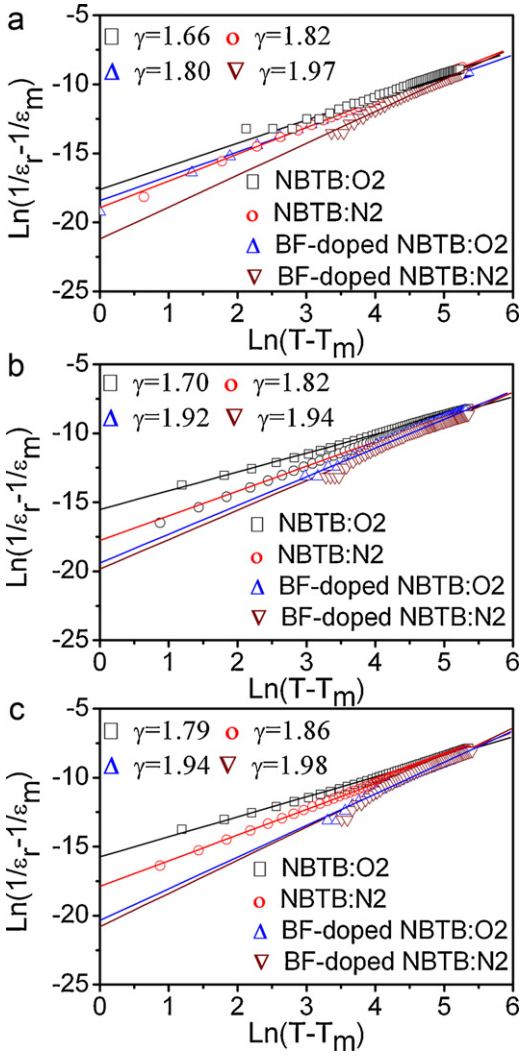

Fig. 5. Plots of $\mathrm{Ln}(1/\varepsilon_r - 1/\varepsilon_m)$ versus $\mathrm{Ln}(T - T_m)$ for the NBTB and BF-doped NBTB ceramics sintered in different atmospheres at frequencies of 10 kHz (a), 100 kHz (b) and 1 MHz (c). The symbols denote experimental data, while the solid lines denote least-square fitting curves to the modified Curie–Weiss law.

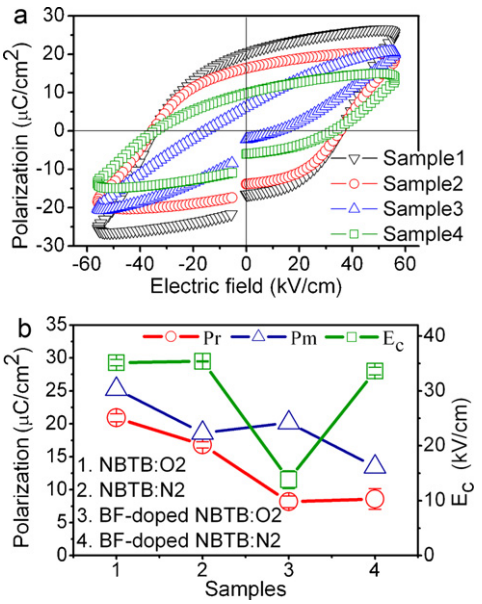

Fig. 6. *P–E* loops of the NBTB and BF-doped NBTB ceramics sintered in different atmospheres measured at 50 Hz (a), and variation of P_r, P_m and E_c for different samples (b).

in N_2 should be the highest. Relative amount of tetragonal phase was different for the ceramics sintered in different atmospheres. Thus, main factors influencing ferroelectric properties of the NBTB and BF-doped NBTB ceramics are oxygen vacancy concentration, A-site vacancy concentration and relative amount of tetragonal phase.

To our knowledge, a decrease in oxygen vacancy concentration and increases in A-site vacancy concentration and percentage of tetragonal phase would facilitate the movement of ferroelectric domains and improve ferroelectric properties [17,20,40–42]. After sintering in N_2, the samples would have lower relative amount of tetragonal phase and A-site vacancy concentration, but higher oxygen vacancy concentration. All these would decrease polarization and increase coercive field. This is the reason why the ceramics sintered in N_2 have smaller polarization and higher coercive field compared to those sintered in O_2. It should be noted that E_c of the BF-doped NBTB ceramics sintered in O_2 was the lowest. Although oxygen vacancy concentration will increase by doping $BiFeO_3$, the BF-doped NBTB ceramics would have decreased oxygen vacancy concentration when they were sintered in O_2. The percentage of tetragonal phase in the BF-doped NBTB ceramics sintered in O_2 (42.9%) is similar to that in the NBTB ceramics sintered in N_2 (42.5%). The ceramics sintered in O_2 would have increased concentrations of A-site vacancy as compared to those sintered in N_2. All these would decrease coercive field. Therefore, the E_c of the BF-doped NBTB ceramics sintered in O_2 was lower than that of the NBTB sintered in N_2. At present, it is unclear whether or not A-site vacancy concentration in the BF-doped NBTB ceramics sintered in O_2 is higher than that in the NBTB ceramics sintered in O_2. We think that the lowest E_c of the BF-doped NBTB ceramics sintered in O_2 could be attributed to a competing effect among A-site vacancy concentration, oxygen vacancy concentration and percentage of tetragonal phase.

4. Conclusions

Effects of sintering atmospheres on microstructures, dielectric and ferroelectric properties of the NBTB and BF-doped NBTB ceramics were studied. The NBTB sintered in O_2, NBTB in N_2, BF-doped NBTB in O_2, and BF-doped NBTB in N_2, had relative amounts of tetragonal phase of 49.8%, 42.5%, 42.9% and 36.1%, respectively. Their mean grain sizes were 2.41, 3.76, 3.68 and 5.06 μm, respectively. The BF-doped NBTB ceramics sintered in N_2 consisted of grains with round edges and corners, while the ceramics sintered in O_2 consisted of cube-shaped grains with sharp edges and corners. The NBTB and BF-doped NBTB ceramics sintered in N_2 showed weakened dielectric anomalies corresponding to the phase transition between ferroelectric phase and the so-called "intermediate phase". At the same time, they had increased ε_m values, enhanced degree of diffuseness of the phase transition between the "intermediate phase" and paraelectric phase, and decreased T_m values. The difference in dielectric properties between the ceramics sintered in different atmospheres was closely related to their difference in oxygen vacancy concentration. It can be concluded that ferroelectric properties of a ferroelectric ceramic with coarse grains are determined concurrently by oxygen vacancy concentration, A-site vacancy concentration and percentage of tetragonal phase. Our work has shown that oxygen vacancy played a very important role in determining microstructures, dielectric and ferroelectric properties of the NBTB-based ceramics.

Acknowledgements

This work was supported by the National Natural Science Foundation of China (No. 11004127), Fundamental Research Funds for the Central Universities (No. GK200902054), Laboratory Opening-Found for College Students in Shaanxi Normal University and Shaanxi Normal University Work-Study Programme for Scientific Research Innovation Fund.

References

[1] H.I. Hsiang, L.T. Mei, Y.J. Chun, J. Am. Ceram. Soc. 92 (2009) 2768–2771.
[2] Y.J. Dai, S.J. Zhang, T.R. Shrout, X.W. Zhang, J. Am. Ceram. Soc. 93 (2010) 1108–1113.
[3] Y.S. Sung, J.M. Kim, J.H. Cho, T.K. Song, M.H. Kim, T.G. Park, Appl. Phys. Lett. 96 (2010) 202901∼1–1202901∼3.
[4] M. Cernea, E. Andronescu, R. Radu, F. Fochi, C. Galassi, J. Alloys Compd. 490 (2010) 690–694.
[5] D.Z. Zhang, X.J. Zheng, X. Feng, T. Zhang, J. Sun, S.H. Dai, L.J. Gong, Y.Q. Gong, L. He, Z. Zhu, J. Huang, X. Xu, J. Alloys Compd. 504 (2010) 129–133.
[6] M.L. Liu, Y.F. Qu, D.A. Yang, J. Alloys Compd. 503 (2010) 237–241.
[7] C.W. Tai, Y. Lereah, Appl. Phys. Lett. 95 (2009) 062901–062903.
[8] S.N. Yun, X.L. Wang, J. Shi, D.L. Xu, J. Alloys Compd. 485 (2009) 610–615.
[9] X. Tan, E. Aulbach, W. Jo, T. Granzow, J. Kling, M. Marsilius, H.J. Kleebe, J. Rödel, J. Appl. Phys. 106 (2009) 044107∼1–144107∼7.
[10] J.E. Daniels, W. Jo, J. Rödel, V. Honkimäki, J.L. Jones, Acta Mater. 58 (2010) 2103–2111.
[11] S.T. Zhang, A.B. Kounga, W. Jo, C. Jamin, K. Seifert, T. Granzow, J. Rödel, D. Damjanovic, Adv. Mater. 21 (2009) 1–5.
[12] Q.H. Zhang, Y.Y. Zhang, F.F. Wang, Y.J. Wang, D. Lin, X.Y. Zhao, H.S. Luo, W.W. Ge, D. Viehland, Appl. Phys. Lett. 95 (2009) 102904∼1–1102904∼3.
[13] P. Fu, Z.J. Xu, R.Q. Chu, W. Li, G.Z. Zang, J.G. Hao, Mater. Sci. Eng. B 167 (2010) 161–166.
[14] Z. Yu, V.D. Krstic, B.K. Mukherjee, J. Mater. Sci. 42 (2007) 3544–3551.
[15] G.A. Smolenskii, I. Chupis, Sov. Phys. Usp. 25 (1982) 475–493.
[16] V. Dorcet, P. Marchet, G. Trolliard, J. Eur. Ceram. Soc. 27 (2007) 4371–4374.
[17] E.V. Ramana, S.V. Suryanarayana, T.B. Sankaram, Solid State Sci. 12 (2010) 956–962.
[18] M.J. Zou, H.Q. Fan, L. Chen, W.W. Yang, J. Alloys Compd. 495 (2010) 280–283.
[19] C.R. Zhou, X.Y. Liu, W.Z. Li, C.L. Yuan, Mater. Chem. Phys. 114 (2009) 832–836.
[20] X.M. Chen, X.X. Gong, T.N. Li, Y. He, P. Liu, J. Alloys Compd. 507 (2010) 535–541.
[21] Y.I. Jung, S.Y. Choi, S.J.L. Kang, Acta Mater. 54 (2006) 2849–2855.
[22] J.G. Fisher, S.J.L. Kang, J. Eur. Ceram. Soc. 29 (2009) 2581–2588.
[23] J.G. Fisher, D. Rout, K.S. Moon, S.J.L. Kang, J. Alloys Compd. 479 (2009) 467–472.
[24] J.G. Fisher, D. Rout, K.S. Moon, S.J.L. Kang, Mater. Chem. Phys. 120 (2010) 263–271.
[25] S.W. Zhang, H.L. Zhang, B.P. Zhang, G.L. Zhao, J. Eur. Ceram. Soc. 29 (2009) 3235–3242.
[26] X.P. Jiang, L.Z. Li, M. Zeng, H.L.W. Chan, Mater. Lett. 60 (2006) 1786–1790.
[27] I. Fujii, M. Ugorek, Y. Han, S. Trolier-McKinstry, J. Am. Ceram. Soc. 93 (2010) 1081–1088.
[28] T. Takenaka, K. Maruyama, K. Sakata, Jpn. J. Appl. Phys. 30 (1991) 2236–2239.
[29] S.E. Park, S.J. Chung, J. Am. Ceram. Soc. 79 (1996) 1290–1296.
[30] A. Tkach, P.M. Vilarinho, A.L. Kholkin, Acta Mater. 54 (2006) 5385–5391.
[31] K. Uchino, E. Sadanaga, T. Hirose, J. Am. Ceram. Soc. 72 (1989) 1555–1558.
[32] S. Lee, C.A. Randall, Z.K. Liu, J. Am. Ceram. Soc. 90 (2007) 2589–2594.
[33] X.M. Chen, P. Liu, J.P. Zhou, W.W. Kong, J.W. Zhang, Physica B 405 (2010) 2815–2819.
[34] E. Salje, U. Bismayer, B. Wruck, J. Hensler, Phase Transit. 35 (1991) 61–74.
[35] K.H. Härdtl, R. Wernicke, Solid State Commun. 10 (1972) 153–157.
[36] K. Uchino, S. Nomura, Ferroelectrics 44 (1982) 55–61.
[37] C.R. Zhou, X.Y. Liu, W.Z. Li, C.L. Yuan, Solid State Commun. 149 (2009) 481–485.
[38] W.R. Buessem, L.E. Cross, A.K. Goswami, J. Am. Ceram. Soc. 49 (1966) 33–36.
[39] A. Shigemi, T. Wada, Jpn. J. Appl. Phys. 43 (2004) 6793–6798.
[40] W. Wang, J. Zhu, X.Y. Mao, X.B. Chen, Mater. Res. Bull. 42 (2007) 274–280.
[41] T. Friessnegg, S. Aggarwai, R. Ramesh, B. Nielsen, E.H. Poindexter, D.J. Keeble, Appl. Phys. Lett. 77 (2000) 127–129.
[42] I. Coondoo, S.K. Agarwal, A.K. Jha, Mater. Res. Bull. 44 (2009) 1288–1292.